Appl. Phys. A 62, 51–59 (1996)

Applied Physics A Materials Science & Processing

Nanosecond-time-resolution thermal emission measurement during pulsed excimer-laser interaction with materials

X. Xu[1,*], C.P. Grigoropoulos[1,], R.E. Russo[2]**

[1] Department of Mechanical Engineering, The University of California, Berkeley, CA 94720, USA
(Fax: + 1-510/642-6163, E-mail: CGRIGORO@euler.berkeley.edu
[2] Energy and Environmental Division, Lawrence Berkeley Laboratory, Berkeley, CA 94720, USA

Received: 10 October 1994/Accepted: 8 June 1995

Abstract. A nanosecond-time-resolution pyrometer has been developed for measuring the transient surface temperature of a solid material heated by pulsed excimer-laser irradiation. Fast germanium diodes are employed to capture the transient thermal emission signals in the wavelength range between 1.2 and 1.6 μm. The surface temperature is derived from the measured spectral thermal emission. The directional spectral emissivity is determined in situ by measuring the transient directional spectral reflectivity and applying Kirchhoff's law. The experimental results are in good agreement with numerical thermal modeling predictions. The pyrometric thermal emission measurement also yields the solid/liquid interface temperature during the pulsed excimer-laser-induced melting. The relation between the measured interface superheating temperature and the interface velocity reveals the melting kinetic relation during the high-power, short-pulse laser-induced phase-change processes.

PACS: 44.10. + i; 64.70.Dv; 79.20.Ds

Excimer lasers, having pulse durations between 10 and 30 ns and operating at ultraviolet wavelengths, have been at the forefront of laser research in the past decade. The development of new excimer-laser-based applications continues to progress at a rapid pace. The most notable research applications utilize the excimer laser as an energy source in surface treatment and in pulsed laser deposition of a variety of novel thin films. To improve the quality of the process, control of the temperature field induced by the excimer-laser beam becomes crucial. Development of robust, in situ, non-contact temperature measurement techniques is necessary for advancing laser-assisted material processing methods. On the other hand, it has been shown [1] that the physical phenomena are much more complicated when the incident laser energy density is sufficient to cause material removal. The exact mechanism of energy coupling between the laser and the target material in the laser ablation process remains unclear. The surface temperature measurement is an important issue for the fundamental study of the laser–material interaction.

Several techniques have been developed to obtain the transient temperature field during pulsed laser processing. A classical time of flight measurement was used to measure the lattice temperature of bulk crystalline silicon during pulsed ruby laser heating [2]. In this method, the kinetic energy of particles released from the surface of the material is measured. However, the derivation of the temperature is based on the assumption that the ejected particles are in a thermal equilibrium state. Such an assumption may not be valid, particularly when the sputtering mechanism is non-thermal. Transient temperature during nanosecond pulsed laser irradiation was

*Current address: School of Mechanical Engineering, Purdue University, West Lafayette, IN 47907, USA
**To whom all correspondence should be addressed

Abbreviations:
C_1, blackbody radiation constant, $C_1 = 3.7420 \times 10^8$ W μm^4/m^2; C_2, blackbody radiation constant, $C_2 = 1.4388 \times 10^4$ μm K; C_p, specific heat in J/kg K; dA, area on the laser-heated spot whose thermal emission is detected in mm^2; D, Detector responsivity in A/W; $e_{\lambda b}$, blackbody spectral emissive power in W/m^2 μm; f, focal length of lens in mm; F, laser fluence in J/cm^2; i, complex imaginary unit ($i = \sqrt{-1}$); K, thermal conductivity in W/m K; L, latent heat in J/kg; M, minimization function to calculate the temperature from thermal emission in (6) and (10); $\tilde{n}$, complex refractive index; R, reflectivity; R_s, specular reflectivity; R_d, diffuse reflectivity; T, temperature in K; T_{eff}, effective temperature (7) in K; T_{int} interface temperature in K; T_m, equilibrium melting temperature in K; V, voltage recorded on the oscilloscope in V; V_{int}, velocity of the solid/liquid interface in m/s; W, impedance of the oscilloscope in Ω
Superscript: i, directional
Subscripts: c, calculated results; exc, excimer laser; ℓ, liquid silicon; m, measured results; qz, quartz substrate; s, solid silicon; λ, spectral quantity
Greek symbols:
α, absorptivity; ΔT, interfacial superheating temperature, $\Delta T = T_{int} - T_m$ in K; ε, emissivity; θ, polar angle; Θ, angle of light incidence; λ, wavelength in μm; ρ, density in kg/m^3; τ, transmissivity of optics; ϕ, Azimuthal angle

also measured using an iron-constantan thin-film thermocouple [3] and a thin-film thermistor [4]. The complicated sample preparation involved in these two methods limits their usefulness for direct non-contact temperature monitoring of materials. The optical reflectivity technique is the most widely used method to study the pulsed laser-induced phase transformation [5, 6], and probe the transient temperature field [7]. To obtain the temperature information by the optical reflectivity method, the temperature dependence of the optical properties (i.e., the complex refractive index) must be known. The sensitivity of this optical technique is reduced as the variation of the reflectivity with temperature is decreased.

In this work, it is intended to develop a nanosecond-time-resolution, pyrometer-type temperature measurement technique for the detailed quantitative study of pulsed laser–material interactions. The initial work is published elsewhere [8]. The nanosecond-time-resolution pyrometer is designed to operate in the spectral range between 1.2 and 1.6 μm. The test sample is a thin polycrystalline silicon (p-Si) film deposited on a quartz substrate. The spectral directional emissivity of the p-Si film is determined in situ, by measuring the transient directional spectral reflectivity and applying Kirchhoff's law. The measured temperature field is compared with the results of numerical heat transfer modeling. It is noticed that the fastest pyrometer reported in the literature operates in the microsecond time scale [9].

The pyrometer is also used to study the solid/liquid interface kinetic relation during the excimer-laser-induced phase transformation. Since the melting front velocity induced by excimer laser is on the order of meters per second, the phase change is no longer expected to be an equilibrium process, and the assumption of a constant, thermodynamic equilibrium phase-change temperature is no longer valid. Interface kinetic theory [10] describes the relation between the interface superheating/undercooling temperature and the interface velocity. Experimental study of the interface kinetic relation requires measurement of both the interface velocity and the interface temperature. Direct measurement of the temperature at the solid/liquid interface during excimer-laser-induced melting is accomplished by using samples of suitable structure and optical properties. In earlier work [11], the electric conductance method was used to determine the interface velocity and the melting process was modeled numerically. Comparison between modeling and experiment demonstrated good agreement, thus proving that the melting front propagation can be described by heat transfer analysis. In this work, the measured melting interface temperature, combined with the calculated interface velocity, is used to study the interface kinetic relation.

1 Description of the experimental procedure

Figure 1 shows the experimental setup for this study. A pulsed KrF excimer laser ($\lambda_{exc} = 0.248$ μm) is used as the heating source. The Full-width-Half-Maximum (FWHM) pulse duration of the excimer-laser beam is measured to be 26 ns, using a fast silicon PIN photodiode

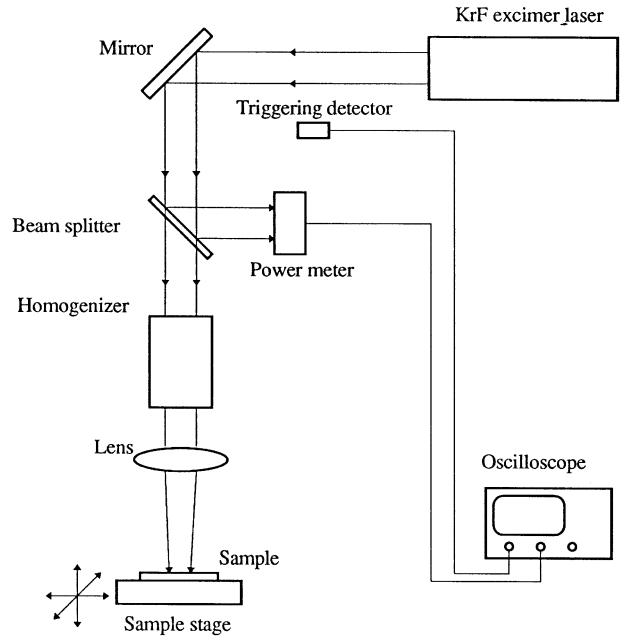

Fig. 1. Experimental setup for pulsed excimer-laser processing of p-Si films

with 1 ns rise/fall time, and a digitizing storage oscilloscope with 1 GHz bandwidth operated at single-shot acquisition mode (1 ns time resolution). The laser pulse energy is monitored by an energy meter which receives the laser light reflected from a beam splitter. Pulse-to-pulse energy variation is about 10%. The excimer-laser beam is focused onto the sample surface in the normal direction. A beam homogenizer is used to ensure the spatial uniformity of the laser beam. The variation of the laser light intensity on the sample surface is less than 10% over the central 90% portion of the laser beam.

The sample is a thin polycrystalline silicon (p-Si) layer on a fused quartz substrate. The p-Si film was deposited by low-pressure chemical vapor deposition (LPCVD), at a temperature of 605 °C and a pressure of 300 mTorr. The thickness of the p-Si film is 0.5 μm.

The pyrometer is designed to operate in the temperature range between 1500 and 3000 K. In this temperature range, the thermal emission is strongest at wavelengths between 1 and 2 μm, according to Wien's displacement law. To measure the thermal emission at nanosecond time scale, it is important to increase the signal level and the detection system responsivity. Germanium diodes (EG&G Judson, J16-18A-R01M-HS) are chosen to detect the emission signals since the active spectral range of these diodes extends from 0.8 to 1.8 μm. The active sensing area of the germanium diode is 1 mm^2. The germanium diode is reversely biased to obtain a 1 ns time resolution. The electric signal from the germanium diode is recorded on the digitizing oscilloscope.

A large solid angle is also required to achieve maximum energy collection efficiency. Lenses with short focal lengths and large diameters are desirable. Two 2-in diameter lenses with focal lengths of 65 mm are chosen to image the center area of the laser-heated spot onto the

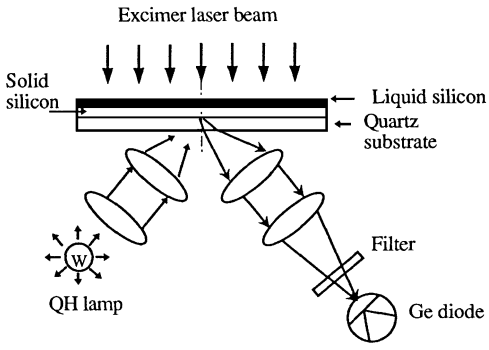

Fig. 2. Experimental setup for transient thermal emission and emissivity measurement

active area of the germanium diode. Low-fluorescence fused-quartz lenses are used to minimize the excimer light-induced fluorescence. Due to the symmetry of the arrangement of the collecting optical components between the sample surface and the germanium diode, the germanium diode senses the thermal emission from an area $dA = 1\ mm^2$ at the center of the heated spot.

Band pass filters in the wavelength range from 1.2 to 1.6 μm, having bandwidths of approximately 0.08 μm, are used to distinguish spectral thermal emission signals. Thermal emission is measured at four different wavelengths (1.2, 1.4, 1.5, and 1.6 μm) to enhance the measurement accuracy. The spectral transmission characteristics of the filters, as well as the spectral response of the germanium detectors, are calibrated.

To measure the temperature of the solid/liquid interface during laser melting of the p-Si sample, thermal emission is collected from the *back* side of the sample, as shown in Fig. 2. The Quartz Halogen (QH) lamp is used for reflectivity measurement as discussed below. A beam splitter can be placed between the two focusing lenses to form images onto two germanium diodes. In this way, thermal emission signals at different wavelengths can be recorded simultaneously. In the wavelength range between 1.2 and 1.6 μm, both the solid silicon and the quartz substrate are transparent, so that their emissivity is zero according to Kirchhoff's law. The thermal emission from the solid silicon film and the quartz substrate in this wavelength range is insignificant. However, when the surface of the p-Si film is melted by the pulsed laser beam, the thermal emission from liquid silicon is detectable, since the liquid silicon has an emissivity around 0.28 in the near-IR. Thus, the measured thermal emission signal is ascribed to liquid silicon. At near IR wavelengths, the radiation absorption depth in liquid silicon is less than 18 nm. Therefore, the thermal radiation is emitted from a thin liquid silicon layer just behind the solid/liquid interface. The temperature derived from the measured thermal emission is close to the solid/liquid interface temperature. (The effect of a temperature gradient within the 18 nm absorption depth on the emitted radiation intensity is discussed later.) The temperature of the moving solid/liquid interface is measured in the experiment. The maximum melting depth achieved is less than 0.4 μm, which is more than five orders of magnitude smaller than the focal lengths of the lenses ($f = 65$ mm). The effect of the interface movement on the energy collection (i.e. depth of field effect) is therefore entirely negligible.

To obtain temperature information from the measured thermal emission, the temperature dependence of the spectral emissivity is required. The emissivity varies with temperature, wavelength and surface conditions. The emissivity of a real sample surface can be much different from the reported literature data obtained for "ideal" surfaces under strictly controlled experimental conditions. In this work, the emissivity of the sample is independently measured. Figure 2 also illustrates the experimental setup for measurement of the transient reflectivity during pulsed excimer-laser heating. The temporal evolution of the emissivity can be obtained from transient reflectivity measurement (see the next section). In the transient reflectivity measurement, a 100 W QH lamp is used as the light source. The light from the QH lamp is focused onto the sample surface by two lenses. The reflected portion of this beam is refocused by lenses onto the germanium diode and recorded by the oscilloscope. Band pass filters (the same as those used in the thermal emission measurement) are used to measure the reflectivity at different wavelengths. The measured reflectivity signal also includes the thermal emission from the sample. Two measurements are taken at each wavelength and laser fluence, the first of thermal emission only (with the QH lamp off) and the second of the simultaneously recorded thermal emission and reflection. The reflectivity is obtained by subtracting the thermal emission signal from the combined signal. The room temperature absolute reflectivity is calibrated with a metallic mirror (ER.2, Newport) which has a reflectivity greater than 97% at near-IR wavelengths. In order to eliminate the effect of the laser energy instability, the fluence of each laser shot is measured. The experimental data are accepted when the measured laser fluence is close to the desired value. The surface of the sample shows little change from shot-to-shot for the laser fluences used in this experiment.

2 Theoretical background

The derivation of temperature from thermal emission measurement is based on Planck's blackbody radiation intensity distribution law [12]:

$$e_{\lambda b} = \frac{2\pi C_1}{\lambda^5 \exp(C_2/\lambda T) - 1}. \tag{1}$$

In the above expression, $e_{\lambda b}$ is blackbody emissive power, λ is wavelength, T is temperature, and C_1 and C_2 are blackbody radiation constants. The strong UV radiation of the excimer laser could trigger fluorescence from optical components. The effect of the fluorescence in the experiment is examined (see below), and is found to be negligible.

The detector collects thermal radiation through a solid angle (θ_1 to θ_2, ϕ_1 to ϕ_2) and over a wavelength bandwidth (λ_1 to λ_2). In fact, the voltage signal recorded on the oscilloscope, V, represents an integration of the thermal emission in this solid angle and wavelength band,

modified by the emissivity of the material, the transmission of the optical components, and the detector spectral response:

$$V = W/\pi \int_{\lambda_1}^{\lambda_2}\int_{\theta_1}^{\theta_2}\int_{\phi_1}^{\phi_2} \varepsilon'_\lambda(\lambda,\theta,\phi,T)\,\tau(\lambda)D(\lambda)e_{\lambda b}(\lambda,T)\,\mathrm{d}\phi\,\mathrm{d}\theta\,\mathrm{d}\lambda\,\mathrm{d}A\,. \quad (2)$$

In the above equation, W is the impedance of the oscilloscope (50 Ω); $\tau(\lambda)$ is the spectral transmittance of the lenses and filters in the optical path; $D(\lambda)$ is the responsivity of the germanium diode at different wavelengths (in units of A/W); $\varepsilon'_\lambda(\lambda, \theta, \phi, T)$ is the directional spectral emissivity; and $\mathrm{d}A$ is the area on the sample that is sensed by the germanium diode.

The emissivity is deduced from transient reflectivity measurement. Invoking Kirchhoff's law, the spectral directional emissivity is equal to the spectral directional absorptivity:

$$\varepsilon'_\lambda(\lambda, \theta, \phi, T) = \alpha'_\lambda(\lambda, \theta, \phi, T)\,. \quad (3)$$

For an opaque, non-transmitting material (such as liquid silicon thicker than about 40 nm), the directional spectral absorptivity can be expressed as

$$\alpha'_\lambda(\lambda, \theta, \phi, T) = 1 - R'_s(\lambda, -\theta, \phi, T) - R_d(\lambda, T), \quad (4)$$

where $R'_s(\lambda, -\theta, \phi, T)$ is the specular reflectivity and $R_d(\lambda, T)$ is the diffuse reflectivity. The measured RMS surface roughness of the samples used in the experiment was within 50 Å, implying optical smoothness. Also, the melting interface is assumed to be optically smooth. Consequently, it can be argued that the diffuse reflection from the sample surface or the melting interface is negligible compared with the specular reflection. In this case, the emissivity can be expressed as

$$\varepsilon'_\lambda(\lambda, \theta, \phi, T) = 1 - R'_s(\lambda, -\theta, \phi, T)\,. \quad (5)$$

The emissivity is derived using the measured transient reflectivity data in (5). Once the emissivity is determined and the thermal radiation emission of the target material is measured, the temperature can be obtained by solving (2).

As stated previously, to enhance the measurement accuracy the thermal emission is measured at four different wavelengths (1.2, 1.4, 1.5, and 1.6 μm). The measured voltage signals at these four wavelengths, $V_{m1.2}$, $V_{m1.4}$, $V_{m1.5}$, and $V_{m1.6}$, are compared with the corresponding calculated values from (2), $V_{c1.2}$, $V_{c1.4}$, $V_{c1.5}$, and $V_{c1.6}$:

$$M(T) = \left|\frac{V_{m1.4}}{V_{m1.2}} - \frac{V_{c1.4}}{V_{c1.2}}\right| + \left|\frac{V_{m1.5}}{V_{m1.2}} - \frac{V_{c1.5}}{V_{c1.2}}\right| + \left|\frac{V_{m1.6}}{V_{m1.2}} - \frac{V_{c1.6}}{V_{c1.2}}\right|. \quad (6)$$

In the above expression, the calculated voltages are functions of the temperature T. The temperature is determined by minimizing the function $M(T)$.

The transient temperature field and the velocity of the solid/liquid interface were calculated using a one-dimensional heat conduction model [11]. A front tracking algorithm was constructed to calculate the melt propagation. The interface kinetic relation was incorporated into the numerical simulation. The calculated melt phase duration and transient melt depth were in agreement with experimental results obtained by the electric conductance method that were also cross-checked via optical reflectivity and transmissivity probing. In this work, the melting durations are calculated and compared with the data determined by in situ optical reflectivity measurement. The complex optical refractive index of the p-Si film at the excimer-laser wavelength ($\lambda_{exc} = 248$ nm) was measured by a Variable Angle Spectral Ellipsometer (VASE), $\tilde{n}_{exc} = 1.2 + \mathrm{i}\,2.8$. The temperature dependence of the thermal properties is given by Touloukian [13]. For solid silicon,

$$K_s(T) = 2.99 \times 10^4/(T - 99)\,\mathrm{W/m\,K},$$

$$\rho_s(T)\,C_{p;s}(T) = (1.474 + 0.17066\,T/300) \times 10^6\,\mathrm{J/m^3\,K}.$$

The silicon latent heat of fusion $L = 1.4 \times 10^6$ J/kg.

The thermal properties of liquid silicon and fused quartz are assumed to be temperature-independent:

$$K_\ell = 67\,\mathrm{W/m\,K}, \quad \rho_\ell = 2540\,\mathrm{kg/m^3}, \quad C_{p;\ell} = 957.5\,\mathrm{J/kg}.$$

$$K_{qz} = 1.4\,\mathrm{W/m\,K}, \quad \rho_{qz} = 2200\,\mathrm{kg/m^3}, \quad C_{p;qz} = 1200\,\mathrm{J/kg}.$$

The optical property of liquid silicon is calculated from Drude theory and compared with the experimental data by Shvarev et al. [14]:

$$\tilde{n} = 1.2 + \mathrm{i}2.9.$$

3 Results and discussion

One concern in the thermal emission measurement is the possibility of detection of fluorescence induced by the intense UV light of the excimer laser. The sample materials tested in the experiment are known to generate negligible fluorescence in the wavelength range of the measurement (1.2–1.6 μm). However, the optics in the experimental setup (i.e., lenses and filters) could fluoresce in the near-IR range, even though they are made of low-fluorescence fused silica. A relatively low level of fluorescence could disturb the thermal emission spectrum and cause an experimental error in determining the temperature. To evaluate the fluorescence effect, the thermal emission from a sample having a Cr/p-Si/quartz structure is measured. This sample was prepared by sputtering a 0.3 μm thick chromium layer on top of the p-Si/quartz sample. When the thermal emission is measured from the back side of the sample, any possible excimer-laser-induced near-IR fluorescence is completely absorbed in the chromium layer (Fig. 3). This is because the optical absorption depth in chromium at near-IR wavelengths is less than 300 Å. The measured signal from the back side of the Cr/p-Si/quartz sample is entirely a thermal emission signal. Due to light refraction, the thermal emission measured from the back side is confined within a narrower solid angle in the substrate than in the ambient air (Fig. 3). However, the thermal emission signal captured by the detector is not reduced significantly, since the blackbody emissive power in a medium having a refractive index $n > 1$ is stronger by a factor of n^2 than that in vacuum.

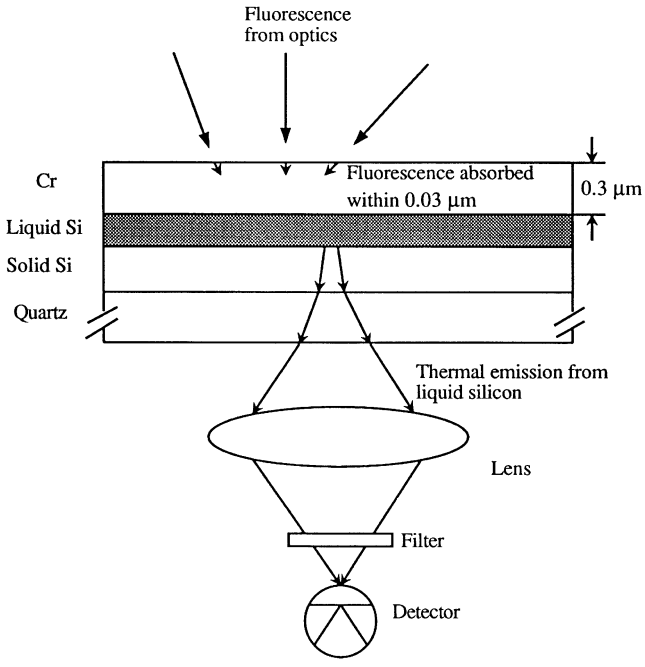

Fig. 3. Absorption of fluorescence by the Cr layer

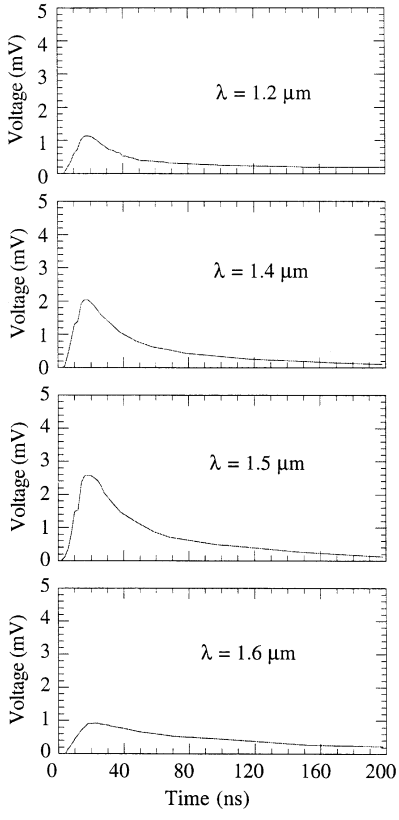

Fig. 4. Measured thermal emission signals from the back side of the Cr/Si/Qz sample, at the laser fluence $F = 0.32\ \mathrm{J/cm^2}$

Figure 4 shows the thermal emission signals at different wavelengths measured from the back side of the Cr/p-Si/quartz sample at a laser fluence of $0.32\ \mathrm{J/cm^2}$. It is recalled that the signal acquired by the detector depends not only on Planck's distribution function $e_{\lambda b}$, but is also modified by the emissivity of the material, ε'_{λ}, the transmissivity of the optics, $\tau(\lambda)$, and the detector responsivity, $D(\lambda)$ (2). A time delay between the start of the laser pulse and the detection of thermal emission can be observed in Fig. 4. This is because it takes a finite time for the back side of the chromium film to reach temperatures producing detectable thermal emission. The temperature reaches a maximum value approximately at the end of the laser pulse. At the laser fluence of $0.32\ \mathrm{J/cm^2}$, the measured maximum temperature is about 1750 K. This temperature exceeds the melting temperature of silicon (1685 K), but is below the melting temperature of chromium (2130 K). It has not been attempted to compare the measured temperature of the Cr/p-Si/quartz sample with numerical predictions, due to the complexity in modeling the three thin-film layer structure, the uncertainties in the thermal properties of the Cr layer, the unknown Cr/p-Si interface structure and its possible effect on the thermal boundary resistance. Prior to silicon melting, the thermal emission emanates from the back side of chromium film, since both solid silicon and quartz are transparent in the wavelength range between 1.2 and 1.6 μm. The thermal emission from the solid silicon film and the quartz substrate in this wavelength range is negligible. When the silicon layer is melted, the temperature measured from the back side of the sample is essentially the temperature of the solid/liquid interface. Therefore the measured maximum temperature of 1750 K is the temperature of the liquid layer close to the solid/liquid interface. The measured data indicate that the solid/liquid interface temperature is *higher* than the equilibrium melting temperature.

Thermal emission signals from the front surface of the Cr/p-Si/Qz sample are also measured and compared with the thermal emission signals obtained from the back side. This is done in order to evaluate the effect of possible fluorescence from the optical components. It is found that the emission signals from the front side of the sample follow a Planckian distribution. The maximum temperature at the chromium surface is found to be 1780 K, at the laser fluence of $0.32\ \mathrm{J/cm^2}$. It is expected that any fluorescence would cause a discernible distortion of the blackbody radiation distribution. Thus it can be concluded that the fluorescence, if any, is small compared with the thermal emission signal.

The experimental and numerical investigation of the interface response is performed using the p-Si/quartz sample. Thermal emission is also measured from the back side of the p-Si/quartz sample. Figure 5 shows the transient thermal emission signals measured from the back side of the p-Si/quartz sample at the wavelength of 1.5 μm for several laser fluences. The thermal emission (and thus the interface temperature) reaches the maximum value several nanoseconds after the initiation of melting. The thermal emission measurement also yields the melting duration, since only liquid silicon emits light in the wavelength range between 1.2 and 1.6 μm. This situation is different from the previously discussed experiment on the Cr/p-Si/quartz sample. In that case, the melting duration could not be obtained from thermal emission measurement, since the Cr film was also a thermal radiation emitter. The length of the arrows in Fig. 5 indicates the duration of the

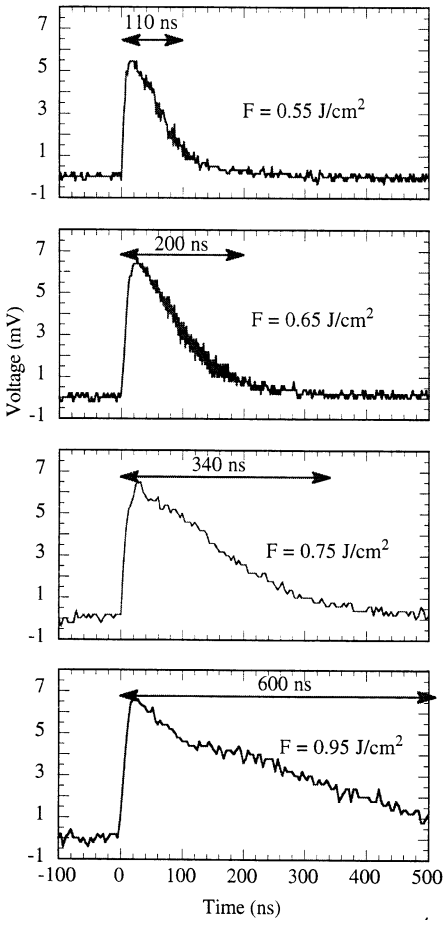

Fig. 5. Thermal emission signals from the back side of the p-Si film at the wavelength $\lambda = 1.5$ μm. The p-Si/quartz sample is heated by excimer-laser pulses of different fluences

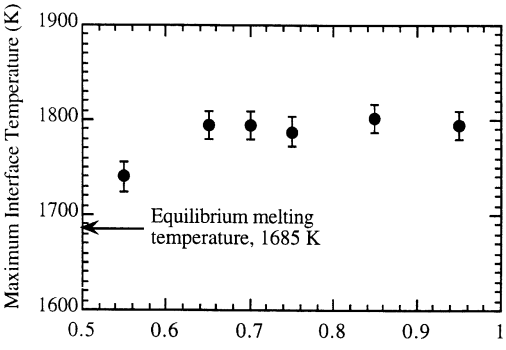

Fig. 6. Maximum melting temperature of the p-Si/quartz sample irradiated by excimer-laser pulses of different fluences

melting process at each laser fluence. Comparing the thermal emission signals at $F = 0.55$ and 0.65 J/cm^2, it can be seen that the maximum interface temperature increases with the laser fluence. However, this trend is not observed for laser fluences higher than 0.65 J/cm^2. The corresponding maximum interface temperatures at different laser fluences are calculated using thermal emission signals at *four* wavelengths (6). In addition, the effect of a temperature gradient at the solid/liquid interface is considered in

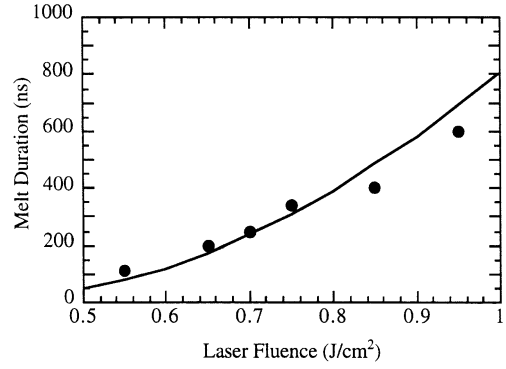

Fig. 7. Comparison between measured and calculated melt durations of the p-Si/quartz sample irradiated by excimer-laser pulses of different fluences

deducing the interface temperature. The measured thermal radiation is emitted from a near-interface liquid layer whose thickness is only a few optical absorption depths. Since there exists a falling temperature gradient in the liquid layer toward the melting interface, the temperature assigned to the measured thermal emission exceeds the interface temperature. Defining the temperature calculated from the thermal emission spectrum as the "effective" temperature, the relation between this effective temperature, T_{eff}, and the temperature distribution inside the liquid film, $T(z)$ is approximated by:

$$\int_{\lambda_1}^{\lambda_2}\int_{\theta_1}^{\theta_2}\int_{\phi_1}^{\phi_2} \varepsilon'_\lambda(\lambda,\theta,\phi,T)\,\tau(\lambda)D(\lambda)e_{\lambda\mathrm{b}}(T_{\mathrm{eff}})\,\mathrm{d}\phi\,\mathrm{d}\theta\,\mathrm{d}\lambda\,\mathrm{d}A$$
$$= \frac{1}{d_{ab}}\int_{0}^{Nd_{\mathrm{ab}}}\int_{\lambda_1}^{\lambda_2}\int_{\theta_1}^{\theta_2}\int_{\phi_1}^{\phi_2} \varepsilon'_\lambda(\lambda,\theta,\phi,T)\,\tau(\lambda)D(\lambda)e_{\lambda\mathrm{b}}(T(z)$$
$$\times \exp\left(-\frac{z}{d_{ab}}\right)\mathrm{d}\phi\,\mathrm{d}\theta\,\mathrm{d}\lambda\,\mathrm{d}z\,\mathrm{d}A\,. \qquad (7)$$

The left-hand side of the above equation has the form established in (2). The right-hand side is the measured thermal emission which originates from a liquid layer of thickness equal to a number ($N = 4$) of optical absorption depths (d_{ab}). The z-coordinate has its origin at the solid/liquid interface, and is directed into the liquid layer. At the highest laser fluence of 0.95 J/cm^2, the temperature gradient at the interface (about 3.3 K/nm) leads to an overestimation of the measured "effective" temperature by approximately 40 K with respect to the actual interface temperature. The effect of the temperature gradient in the liquid layer has been taken into account in Fig. 6 that presents the maximum solid/liquid interface temperatures at different laser fluences.

In Fig. 7, the melting duration obtained from the thermal emission measurement is compared with the numerical simulation results. The comparison verifies that the thermal emission measured from the back side of the sample emanates from liquid silicon only. Surface optical reflectance probing is employed to independently confirm the melting duration measurement and also examine the possibility that *high-temperature solid silicon* can contribute to the thermal emission. The surface reflectivity measurement yields the melting duration because of the

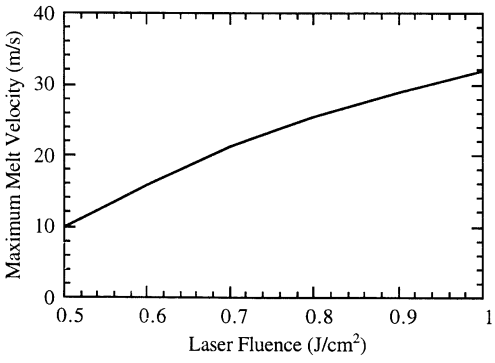

Fig. 8. Calculated maximum melting velocity of the p-Si/quartz sample irradiated by excimer-laser pulses of different fluences

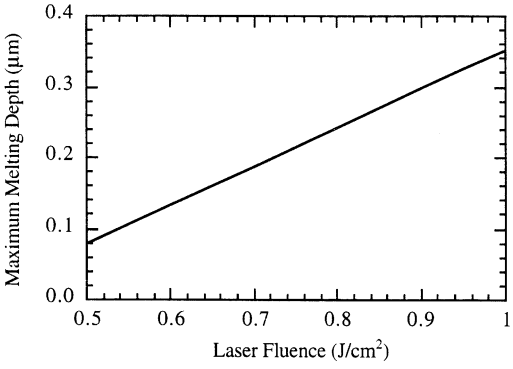

Fig. 9. Calculated maximum melting depth of the p-Si/quartz sample irradiated by excimer-laser pulses of different fluences

large increase of silicon reflectance upon melting. The surface reflectivity and the back side thermal emission measurement results are in close agreement. Considering that any thermal emission from high-temperature solid silicon would have to last much longer than the melted phase, the possibility that the back side thermal radiation is emitted from high-temperature solid silicon is safely dismissed.

Figures 8 and 9 show that the calculated maximum melt front velocities and maximum melting depths increase with the excimer-laser fluence. Numerical calculation also predicted that the maximum surface temperature does not reach the evaporation temperature (2628 K) at the highest laser fluence used in the experiment. The relation between the interface velocity and the interface superheating temperature (Figs. 6 and 8) allows determination of the interface response function during the laser-induced melting process. The melting velocity achieved is on the order of tens of meters per second, suggesting a non-equilibrium process. The relation between the superheating temperature at the solid/liquid interface and the solid/liquid interface velocity is often described by interface kinetic theory [10]:

$$\Delta T_{\text{int}} = C V_{\text{int}}, \tag{8}$$

where ΔT_{int} is the interface superheating temperature, V_{int} is the interface velocity, and C is a material constant. The measured interface superheating temperature combined with the calculated interface velocity provides an experimental study of the interface kinetics under high-power laser irradiation. Assuming that there is a linear relation between the interface superheating temperature and the interface velocity at fluences lower than 0.65 J/cm^2 (more properly, when the interface velocity is below 20 m/s), the response function coefficient C is determined to be about 6 K/(m/s). However, a constant interface temperature is measured at laser fluences higher than 0.65 J/cm^2. The interface response function, (8), is therefore invalid in the high laser fluence regime. When the interface moving velocity is higher than 20 m/s, the interface superheating temperature is "saturated" at about 110 K.

Thermal emission from the top of the sample is also measured to confirm that the surface does not experience boiling. In the case of surface evaporation, the solid/liquid interface velocity increases only slightly with fluence; the excess laser energy is consumed by the latent heat of vaporization. Due to the fact that the optical absorption depth in liquid silicon is less than 18 nm for the wavelength range of 1.2–1.6 μm, the measured thermal emission emanates from the surface skin layer of liquid silicon. The experimental results show that the maximum surface temperature at the laser fluence of 0.95 J/cm^2 is about 2100 K, which is well below the boiling temperature of liquid silicon.

Bulk crystalline silicon is also used as a sample material in this experiment. The surface temperature of a bulk crystalline silicon (c-Si) wafer heated by the excimer-laser light is measured. The advantage of using crystalline silicon as a test material is that the optical and thermal properties are well characterized. The melting threshold of single-crystal silicon is substantially higher than that of the p-Si films since (a) c-Si has higher reflectivity at the excimer-laser light wavelength, and (b) the c-Si sample has a smaller thermal resistance compared with the composite p-Si/quartz sample. At a laser fluence $F = 0.6$ J/cm^2, which is slightly above the melting threshold fluence, the measured maximum temperature is 1900 K. The time interval within which thermal emission is detected yields a melting duration of about 25 ns, since only liquid silicon emits light in the wavelength range from 1.2 to 1.6 μm. The numerical calculation predicts a maximum surface temperature of 1870 K and a melting duration of 22 ns. At another laser fluence F = 0.9 J/cm^2, the measured maximum surface temperature is 2300 K and the melting duration is 60 ns. Numerical calculation for this laser fluence yields correspondingly 2210 K and 73 ns. The optical complex refractive index of c-Si used in the calculation is $\tilde{n} = 1.68 + \text{i}\ 3.58$ [15].

Figure 10 illustrates the transient surface reflectivity signal of the bulk silicon sample at the wavelength of 1.5 μm. The laser fluence is 0.9 J/cm^2 and the probing light angle of incidence $\Theta = 45^\circ$. The reflectivity has a value of 0.54 at room temperature. However, the emissivity of silicon at room temperature is zero since solid silicon is transparent in the wavelength range between 1.2 and 1.6 μm. When the silicon sample is melted by the laser pulse, the reflectivity increases to 0.74. The refractive index of liquid silicon was measured by Shvarev et al. (1975)

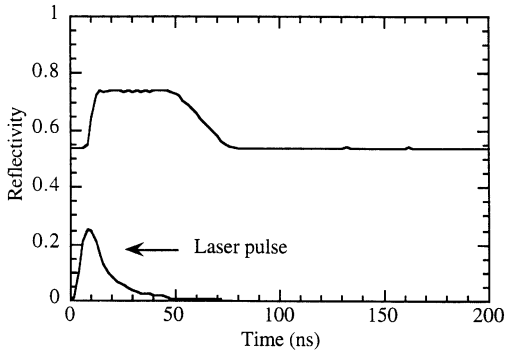

Fig. 10. Transient surface reflectivity of bulk silicon for the wavelength $\lambda = 1.5$ μm, at the laser fluence $F = 0.9$ J/cm^2. The probing angle of incidence $\Theta = 45^\circ$

in the wavelength range between 0.4 and 1.0 μm. The refractive index of liquid silicon at 1.5 μm can be extrapolated from their data, or estimated using free electron Drude theory, to be $\tilde{n} = 7.1 + \mathrm{i}\ 7.2$. This value of the complex refractive index yields a reflectivity of 0.75 at an incident angle of 45°, which is consistent with the measured value, 0.74. The reflectivity is reduced to 0.54 when the sample surface is recrystallized. Using (5), the emissivity of liquid silicon is determined to be $1 - 0.74 = 0.26$, at $\lambda = 1.5$ μm and $\Theta = 45^\circ$. The transient reflectivity of the sample at other wavelengths and incident angles is also measured. However, none of the samples used in this work exhibits strong reflectivity dependence on wavelength. The variation of the measured emissivity is within the experimental uncertainty. This is due to the rather narrow spectral range applied. Calculation of the optical refractive index of liquid Si also indicates that the dependence of liquid Si emissivity on wavelength is weak in the range of 1.2–1.6 μm.

The major source of error in this experiment is introduced by the low level of the transient thermal emission signal collected at the nanosecond time scale. Thus, the signal to noise ratio is relatively low. This affects the accuracy in both the thermal emission measurement and the emissivity measurement. The signal to noise ratio of a typical signal is about 50 when the surface temperature is maximum, yielding an error of about $\pm$ 100 K in absolute temperature determination. This experimental error ($\pm$ 100 K) is large compared with the temperature difference between the measured temperature of the solid/liquid interface and the equilibrium melting temperature. However, differences between thermal emission signals corresponding to different laser fluences can be determined much more accurately. Another way to obtain the temperature and verify the experimental results is by comparing the amplitudes of thermal emission signals acquired at different laser fluences but at a fixed wavelength. Denoting the measured thermal emission signal (i.e., the voltage recorded on the oscilloscope) at the λ_1 wavelength and the laser fluence F_1 to be $V_m(\lambda_1, F_1)$, and the thermal emission signal at the same wavelength and the laser fluence F_2 to be $V_m(\lambda_1, F_2)$, the temperature at the laser fluence F_2 can be derived using the following equation:

$$\frac{V_c(\lambda_1, F_2)}{V_c(\lambda_1, F_1)} = \frac{V_m(\lambda_1, F_2)}{V_m(\lambda_1, F_1)}. \tag{9}$$

The right-hand side of the above equation is the ratio of the measured thermal emission signals at two different laser fluences but at the same wavelength. The subscript "c" indicates the calculation results using (2). The maximum temperature at the laser fluence F_1 (e.g., $F_1 = 0.55$ J/cm^2 for the p-Si sample) is determined from (6). The maximum temperature achieved at the fluence F_2 can then be determined from (9). The accuracy of this procedure is enhanced by considering multiple wavelengths and employing the following minimization function:

$$M(T) = \left|\frac{V_m(\lambda_1, F_2)}{V_m(\lambda_1, F_1)} - \frac{V_c(\lambda_1, F_2)}{V_c(\lambda_1, F_1)}\right| + \left|\frac{V_m(\lambda_2, F_2)}{V_m(\lambda_2, F_1)} - \frac{V_c(\lambda_2, F_2)}{V_c(\lambda_2, F_1)}\right| + \left|\frac{V_m(\lambda_3, F_2)}{V_m(\lambda_3, F_1)} - \frac{V_c(\lambda_3, F_2)}{V_c(\lambda_3, F_1)}\right| + \left|\frac{V_m(\lambda_4, F_2)}{V_m(\lambda_4, F_1)} - \frac{V_c(\lambda_4, F_2)}{V_c(\lambda_4, F_1)}\right|. \tag{10}$$

Using the above equation, the difference between the maximum temperatures at the laser fluences of 0.55 and 0.65 J/cm^2 is determined to be 50 K. This value is consistent with the result obtained from (6). This agreement verifies the validity of the temperature measurement, as well as the observed superheating at the solid/liquid interface.

4 Conclusion

A new pyrometer-type temperature measurement technique with nanosecond time resolution is developed in this work. Transient spectral thermal emission signals in the wavelength range of 1.2–1.6 μm are measured in situ to determine the transient temperature of the material. The temperature measurement range is from about 1500 to 3000 K, with an accuracy of about $\pm$ 100 K. Improving the accuracy of the measurement technique hinges upon the availability of highly sensitive detectors. This temperature measurement technique can be applied to study the transient surface temperature during the pulsed laser interaction with materials.

Transient temperature at the solid/liquid interface during pulsed excimer-laser-induced melting is measured to study the interface response function. It is found that the temperature at the solid/liquid phase-change interface is higher than the equilibrium melting temperature. When the laser fluence is low (lower than 0.65 J/cm^2), the material constant in the interface kinetic relation of the p-Si sample used in this experiment was determined to be 6 K/(m/s). The interface superheating temperature has a maximum value of 110 K when the laser fluence is higher than about 0.65 J/cm^2.

Acknowledgements. Support to this work by the National Science Foundation, under Grant CTS-9210333, is gratefully acknowledged. R. Russo acknowledges the support by the US Department of Energy, Office of Basic Energy Sciences, Division of Chemical Sciences, under contract #DE-AC03-76SF00098. The authors thank Dr. Andrew C. Tam of IBM Almaden Research Center for providing use of experimental facilities. The help of Dr. Hee K. Park and Xiang Zhang of the Department of Mechanical Engineering in carrying out the experimental work is acknowledged.

References

1. C.R. Phipps, R.W. Dreyfus: In *Laser Ionization Mass Analysis*, ed. by A. Vertes, R. Gigbels, F. Adams (Wiley-Interscience, New York 1993) p. 369
2. B. Stritzker, A. Pospieszczyk, J.A. Tagle: Phys. Rev. Lett. **47**, 356 (1981)
3. P. Baeri, S.U. Campisano, E. Rimini, J.P. Zhang: Appl. Phys. Lett. **45**, 398 (1984)
4. J.A. Kittl, R. Reitano, M.J. Aziz, D.P. Brunco, M.O. Thompson: J. Appl. Phys. **73**, 3725 (1993)
5. G.E. Jellison Jr., D.H. Lowndes, D.N. Mashburn, R.F. Wood: Phys. Rev. B **34**, 2407 (1986)
6. I. Lukes, R. Sasik, R. Cerny: Appl. Phys. A **54**, 327 (1992)
7. X. Xu, C.P. Grigoropoulos, R.E. Russo: ASME J. Heat Transfer **117**, 17 (in press)
8. X. Xu, C.P. Grigoropoulos, R.E. Russo: Appl. Phys. Lett. **65**, 1745 (1994)
9. G.M. Foley, M.S. Morse, A. Cezairliyan: In *Temperature, its Measurement and Control in Science and Industry V*, ed. by J.F. Schooley (American Institute of Physics, New York 1982) p. 447
10. K.A. Jackson: In *Crystal Growth and Characterization*, ed. by R. Ueda, J.B. Mullin (North-Holland, Amsterdam 1975) p. 21
11. X. Xu, C.P. Grigoropoulos, R.E. Russo: In *Proc. 6th AIAA/ASME Thermophysics and Heat Transfer Conf.*, Colorado Springs, CO, Vol. HTD 280 (The American Society of Mechanical Engineers, New York 1994) p. 79. ASME J. Heat Transfer **118** (in press)
12. R. Siegel, J.R. Howell: *Thermal Radiative Heat Transfer*, 3rd edn. (Hemisphere, Bristol 1992)
13. Y.S. Touloukian: *Thermophysical Properties of Matter, Thermal Conductivity* (Plenum, New York 1985)
14. K.M. Shvarev, B.A. Baum, P.V. Gel'd: Sov. Phys.-Solid State **16**, 2111 (1975)
15. D.F. Edwards: In *Handbook of Optical Constants of Solids*, ed. by E.D. Palik (Academic, New York 1985) p. 547